Asymmetric Fabry–Perot Oscillations in Metal Grating-Coupled Terahertz Quantum Well Photodetectors

Rong Zhang, Xuguang Guo, Juncheng Cao, and Huichun Liu, *Fellow, IEEE*

***Abstract*— Asymmetric Fabry–Perot oscillations are observed in a high-resolution photocurrent spectrum of a 1-D metal grating-coupled terahertz quantum well photodetector (THzQWP). This behavior is carefully studied through analysis of the field in the device obtained by the finite element method. It is found that such asymmetric oscillation is a pure near-field effect caused by the phase shift of the reflected wave at the grating surface. Our findings also indicate that, because of the long wavelength in the THz range, the near field properties of a microstructured surface could be extracted through the photocurrent measurement on a THzQWP.**

***Index Terms*— Asymmetric Fabry–Perot (FP) oscillation, grating, quantum well photodetector (QWP), terahertz (THz).**

I. Introduction

Subwavelength metallic slits have attracted more and more attention since researchers observed the extraordinary transmission (ET) through subwavelength apertures in metallic films [1]. It is found that the high transmission is due to the excitation of surface plasmons, Fabry–Perot (FP) resonance in the apertures, waveguide mode resonance, or diffraction [2]–[5]. Beruete *et al* [6] performed an analysis of anomalous ET through hole arrays in a rectangular lattice using an equivalent circuit model. Their results are useful to clearly identify the origin of anomalous ET. This model was also used to analyze the anomalous ET in the terahertz (THz) range, and the results showed good agreement between theory and experiment [7]. Lomakin and Michielssen [8] gave a rigorous analysis on the enhanced transmission through metallic plates perforated by arrays of subwavelength holes and sandwiched between dielectric slabs. They attributed the enhanced transmission phenomena to the coupling between the incident plane wave and resonances supported by the perforated plates, that are associated with slow waves. Also, the ET can be explained in terms of Fano interference [9], [10]. Recently, reflection and transmission of thin metallic slit gratings deposited on a dielectric slab are carefully studied in THz range [11], [12]. The results are analyzed by the modal method [13] and can be explained by a pure interference mechanism [12]. However, some near-field information from the evanescent diffracted waves confined at the metal-dielectric interface cannot be detected through the far-field observations such as reflection and transmission measurements.

To detect the surface modes in the THz range, integrated sub-wavelength aperture probe is proposed [14]. Surface plasmon waves can be mapped by this technique, which provides a framework for the analysis of THz near-field images. Thanks to the long wavelength of THz waves, the metal grating coupled terahertz quantum well photodetectors (THzQWPs) [15], [16], with the active region located less than 1 μm below the grating, could be a new option to characterize the near-field effects of the gratings. Constrained by the intersubband transition rule, THzQWPs are insensitive to incident light normal to the as-grown wafer [17]. The method utilizing a grating could bend the light and solve this problem. For normal incident light with frequency below the cutoff (f_c) of the grating (f_c is the frequency where the diffractive angle of the first-order diffracted mode is 90°), the only propagating mode is the zeroth-order diffracted mode with the travelling direction unchanged. Therefore, the propagating mode does not excite any intersubband transition, and the near-field evanescent modes generate the whole photocurrent. In this paper, we report on a high-resolution photocurrent spectral study of a one dimensional (1D) metal grating coupled THzQWP. Asymmetric FP resonances are observed below f_c. This characteristic is numerically studied by the commercial finite element method (FEM) software COMSOL [18]. We find that the asymmetry, which is directly linked to the near-field coupling, is caused by the phase shift at the grating reflection. The result also confirms the feasibility of near-field detection by a THzQWP.

II. Experiments

The metal grating coupled THzQWP studied here is the one from [15] labeled V266-G15. The metal (Ti/Pt/Au, 25/55/300 nm) is fabricated on the top of the device mesa with

Manuscript received February 16, 2012; revised June 19, 2012; accepted June 25, 2012. Date of publication June 29, 2012; date of current version July 18, 2012. This work was supported in part by the 863 Program of China under Project 2011AA010205, the National Natural Science Foundation of China under Grant 61131006, Grant 61021064, and Grant 61176086, the Major National Development Project of Scientific Instrument and Equipment under Grant 2011YQ150021, the Important National Science and Technology Specific Projects under Grant 2011ZX02707, the Chinese Academy of Sciences under Project YYYJ-1123-1, and the Shanghai Municipal Commission of Science and Technology under Project 10JC1417000 and Project 11ZR1444200. The work of H. C. Liu was supported in part by the National Major Basic Research Project under Grant 2011CB925603, and the Shanghai Municipal Major Basic Research Project under Grant 09DJ1400102.

R. Zhang, X. G. Guo, and J. C. Cao are with the Key Laboratory of Terahertz Solid-State Technology, Shanghai Institute of Microsystem and Information Technology, Chinese Academy of Sciences, Shanghai 200050, China (e-mail: rzhang@mail.sim.ac.cn; xgguo@mail.sim.ac.cn; jccao@mail.sim.ac.cn).

H. C. Liu is with the Key Laboratory of Artificial Structures and Quantum Control, Department of Physics, Shanghai Jiao Tong University, Shanghai 200240, China (e-mail: h.c.liu@sjtu.edu.cn).

Color versions of one or more of the figures in this paper are available online at http://ieeexplore.ieee.org.

Digital Object Identifier 10.1109/JQE.2012.2206798

15-μm period grating stripes and 50% filling factor through standard photolithography and lift-off techniques. The f_c of this grating is 5.28 THz. The distance of the active region from the grating is less than half of the detection wavelengths. High-resolution (0.04 cm^{-1}, $\sim$1.2 GHz) photocurrent spectra are measured on a Bomem DA8 spectrometer, and a representative one is given in Fig. 1.

The main response range of V266 is 4.0-6.5 THz [19], fluctuations outside this range shown in Fig. 1(a) should be considered as noise. The noise substantially affects the quality of the spectrum. However, this is the best one that we collected with the limits of the measurement environment, such as mechanical vibration of the cryostat, electrical disturbance from various sources, weak power of the globar source in THz range, and so on. Nevertheless, the asymmetric oscillation still could be seen clearly, Fig. 1(b). We attributed the oscillation to the FP cavity effect of the dielectric slab below the grating [20]. However, as FP resonance in a similar system presented in [11], one would have expected a symmetric behavior in the observed FP modes. In the following, we will show that the asymmetry is a near-field effect, although the far-field FP mode observation is symmetric. We will focus on the range from 4.5 to 5.0 THz, which is below the cutoff of the grating. For those coupling features above the cutoff, detailed discussions are found in [11] and [12].

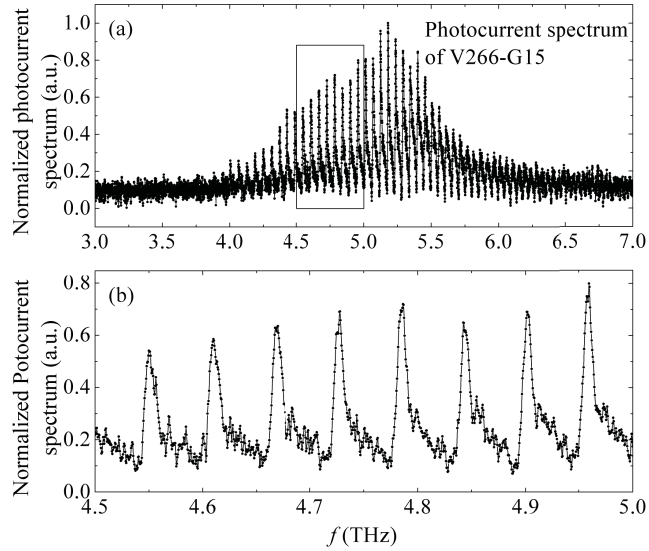

Fig. 1. (a) Normalized photocurrent spectrum of V266-G15 measured at 8 K, with a resolution of 0.04 cm^{-1}. (b) Enlarged view of the box in (a).

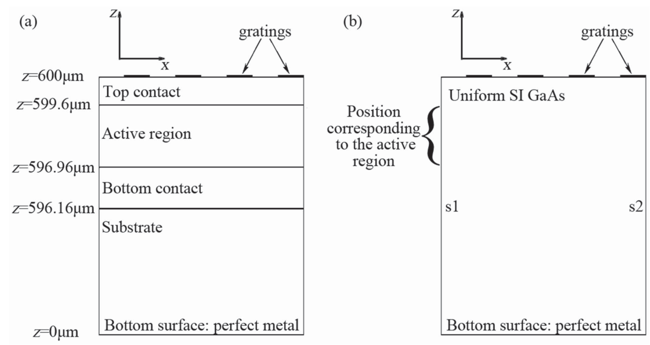

Fig. 2. (a) Schematic of metal grating-coupled THzQWP with all known parameters. The device region is above the substrate. The structure and grating parameters are consistent with V266-G15. (b) Simplified system used in the simulation. A uniform undoped GaAs slab below the grating is considered. The total thickness of the dielectric slab below the grating is 600 μm. The bottom surface is considered a perfect metal. Average $|E_z|^2$ is calculated in the region marked by "Position corresponding to the active region." Schematics (a) and (b) are not drawn to scale.

III. Theoretical Analysis

A. Model

The thickness of the GaAs substrate used for the THzQWP is 600 μm ($\pm$30 μm), and the device is mounted on a copper heat sink by a layer of low-temperature adhesive with unknown thickness and refractive index. For simplification, we start from a model system with all parameters known, as shown in Fig. 2(a). Because the doping densities in the quantum wells and the contacts are relative low, and the Al fraction in the barriers are small, we consider a uniform undoped GaAs slab below the grating, Fig. 2(b). The GaAs slab forms a FP cavity. The copper heat sink is considered as a perfect metal in THz range.

For a p-polarized normal-incident THz plane wave [$\mathbf{E} = (E_x, 0, 0)$, $\mathbf{H} = \left(0, H_y, 0\right)$] with frequency below the f_c of the grating, E_z is finite after diffraction due to evanescent diffracted modes and then causes a photocurrent of the THzQWP. Since E_z is the only effective part in exciting the intersubband transitions, which also corresponds to the surface modes at the metal-dielectric interface, we evaluate the average $|E_z|^2$ in the active region shown in Fig. 2(b). The system is solved by COMSOL 4.2. In the simulation, the refractive index of GaAs is taken from [21]. The loss of GaAs is neglected because the imaginary part of the refractive index of GaAs is nearly 0 in the range from 4.5 to 5 THz. The refractive index of the grating metal is given by the Drude model [13]. Perfect electric conductor boundary condition is set to the bottom surface, and at the sides s1 and s2, periodical boundary condition is applied. The average $|E_z|^2$ is plotted in Fig. 3, and the field distributions at 4.6 THz are given in Fig. 4.

The asymmetric oscillation can be seen clearly in Fig. 3. In Fig. 4, only E_x exists in the far field, which is the zeroth-order diffracted mode. And E_z corresponding to the evanescent diffracted modes falls rapidly with increasing distance away from the grating. Such E_z can be sensed by the THzQWP, and the asymmetry shown in Fig. 3 will be reflected in the photocurrent spectrum.

B. Field Distribution

The near field (E_z) is induced by the propagating wave incident onto the grating. By analyzing the period, it is found that the oscillation is related to the FP resonance of the zeroth-order diffracted mode [20]. To explain the asymmetry, it is necessary to study the intensity of zeroth-order diffracted mode in the vicinity of the grating. Obviously a standing wave will be formed in the FP cavity no matter there is a grating or not, and at the bottom metal surface, it is always a wave node, Fig. 4(left). The standing wave can be expressed as

$$E_x\left(z\right) = A \sin\left(kz\right) e^{-i\left(\omega t - \frac{\pi}{2}\right)} \tag{1}$$

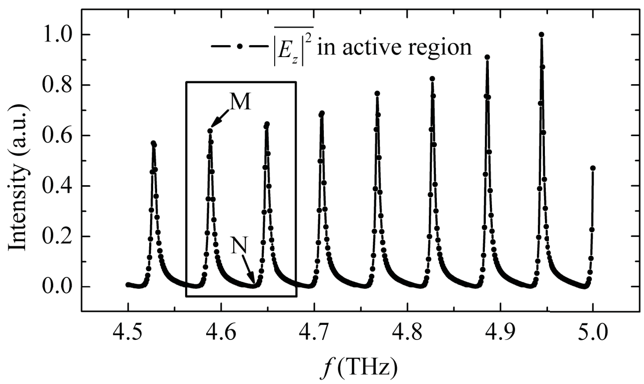

Fig. 3. Normalized oscillations of average $|E_z|^2$ in the active region shown in Fig. 2(b). The grating period is 15 μm, and the filling factor is 50%.

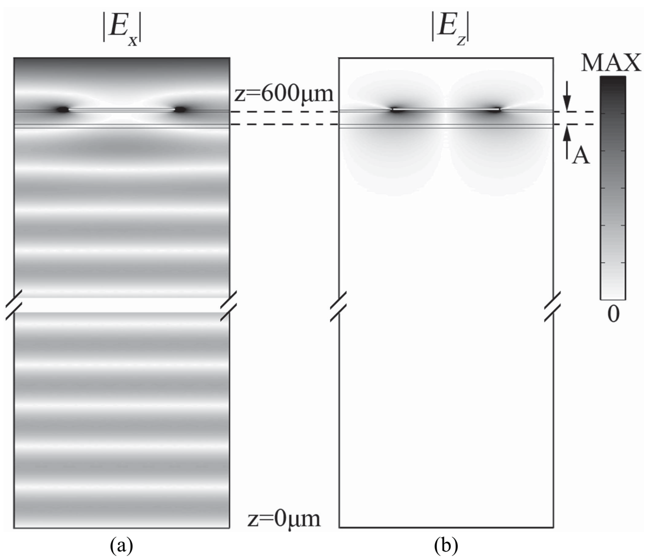

Fig. 4. Field distributions of (a) $|E_x|^2$ and (b) $|E_z|^2$. Marker A indicates the position of the active region. The z direction is drawn to scale.

where $z \in [0, 600]\ \mu$m, $\omega = 2\pi f$, f is the incident frequency, and k is the wave vector in GaAs. The intensity of the standing wave is

$$I(z) \sim |E_x(z)|^2 = [A \sin(kz)]^2. \tag{2}$$

The intensity distribution of the standing wave (zeroth-order diffracted mode) is plotted in Fig. 5(a) for $f = 4.6$ THz.

We define $\varphi(z) = kz$, $\varphi_g = \varphi(z = 600\ \mu\text{m})$, and $I_g = I(z = 600\ \mu\text{m}) \sim A^2 \sin^2 \varphi_g$. Physically, φ_g and I_g are the phase and the intensity of the zeroth-order diffracted mode just below the grating respectively. Fig. 5(b) shows the relation between φ_g (converted into $[0, 2\pi)$) and frequency f.

Below f_c of the grating, all non-zeroth order diffracted modes are evanescent and contribute to the near field E_z. The total intensity of the evanescent modes is proportional to the intensity of the incident light around the grating. Without FP cavity, the zeroth-order diffracted mode will go away from the system. With the FP cavity, this mode will get reflected at the bottom surface and propagate back to the grating. This backward wave interferes with the forward wave, which affects the light intensity around the grating. Here, the intensity, which can be represented by I_g, will be used to analyze the asymmetry in the following.

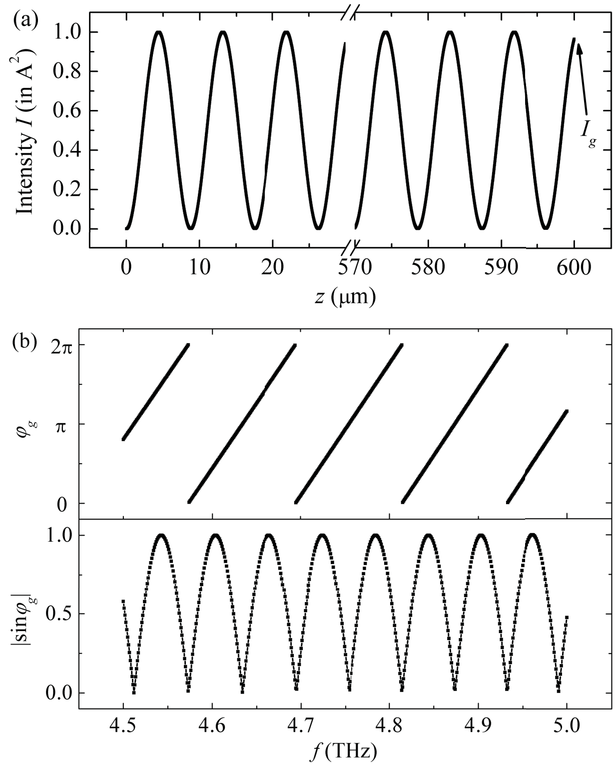

Fig. 5. (a) Normalized intensity distribution of the zeroth-order diffraction mode in the device. (b) φ_g (upper) and $|\sin \varphi_g|$ (lower) versus frequencies.

C. Effective Cavity

For a common FP cavity without grating (Fig. 2 but without grating), the FP resonance condition is

$$2kh + \pi = 2m\pi \tag{3}$$

where h is the length of the cavity, and m is an integer. The additional π on the left-hand side is from the reflection at the bottom metal surface.

For the cavity with gratings shown in Fig. 2, due to the coupling between the metal grating and the dielectric slab, an effective cavity is formed. This case has already been studied in previous publications. In the experiment presented in [11], an additional length is necessary to fit the experimental data; and in [22], by summing up all the "scattering processes," the reflection and transmission of 1D grating are calculated, and a phase shift θ is found after the reflection of the propagating mode at the grating surface. The additional phase shift θ leads to the formation of the effective cavity, and also leads to the asymmetric oscillation in the photocurrent spectrum.

Due to the existence of θ, the FP resonance condition of an effective cavity should be modified as

$$2kh + \pi + \theta = 2m\pi. \tag{4}$$

D. Asymmetric Oscillations

Let us focus on the frequency range from 4.56 THz to 4.68 THz, which contains two oscillation periods within the region marked by a box in Fig. 3. The FP oscillations of the cavities with (effective cavity) and without (original cavity) gratings are given in Fig. 6(b)&(c). These two figures are

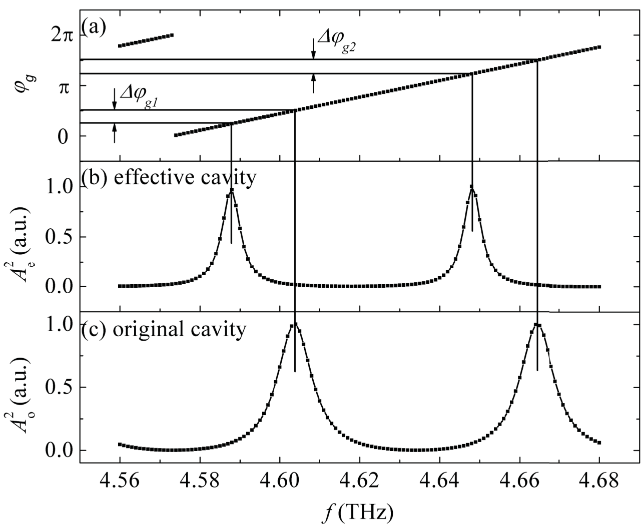

Fig. 6. (a) φ_g, (b) normalized FP resonance of the effective cavity, and (c) normalized FP resonance of the original cavity in the frequency range [4.56, 4.68] THz.

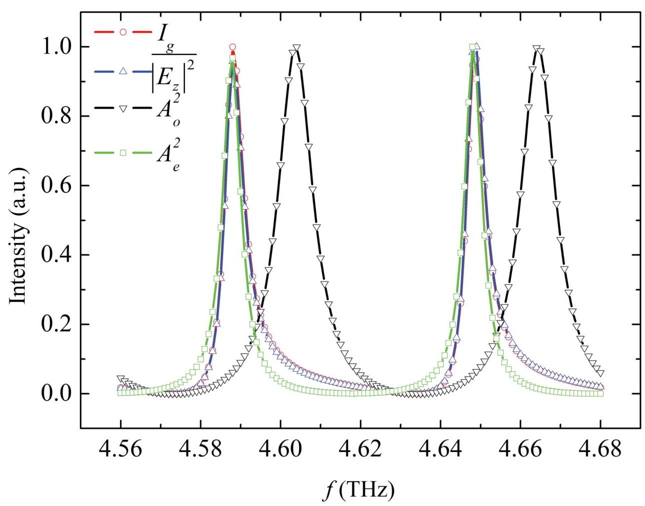

Fig. 7. Comparison of the oscillations of effective cavity (green, open square), original cavity (black, square), I_g (red, open circle), and average $|E_x|^2$ in the active region (blue, circle, from the box in Fig. 3).

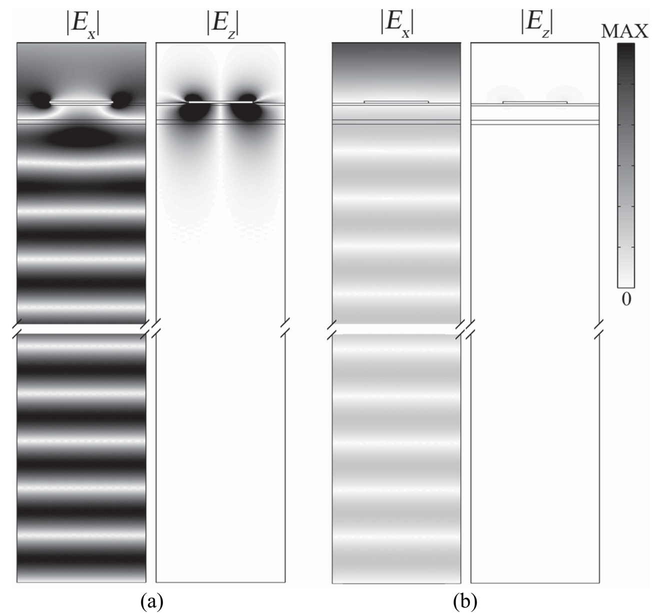

Fig. 8. Field distributions of (a) M: f = 4.588 THz and (b) N: f = 4.634 THz marked in Fig. 3.

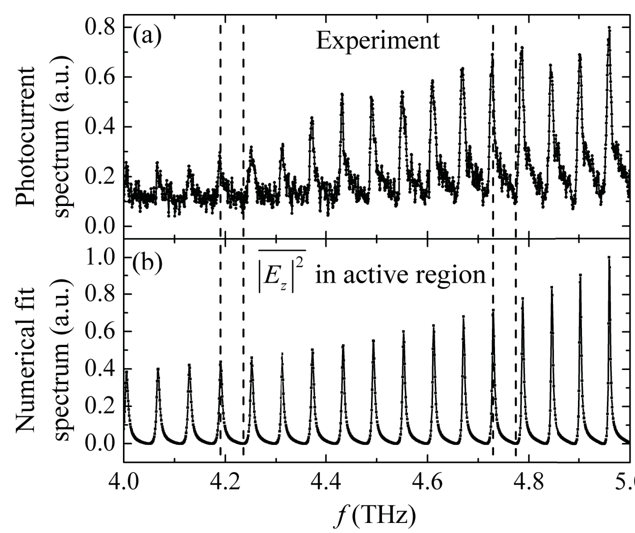

Fig. 9. Comparison of oscillations. (a) Photocurrent spectrum of V266-G15 and (b) average $|E_z|^2$ in the active region of a 614-μm-length cavity.

contrasted by plotting the relation between $A_{o,e}^2$ and frequency f, where A is the amplitude in (1), and the subscripts o and e indicate the original and effective cavities, respectively. It is seen that, as described in (4), the oscillation of the effective cavity is shift from the one of the original cavity. The phase shifts are $\theta_1/2 = \Delta\varphi_{g1} \approx 0.2627\pi$ and $\theta_2/2 = \Delta\varphi_{g2} \approx 0.2644\pi$ respectively, referring to Fig 6(a). It should be mentioned that both FP oscillation curves are symmetric, which confirms that the asymmetry is a pure near-field effect that appears in the oscillation of $|E_z|^2$. Therefore, although the frequency shift can be obtained by far-field measurements such as reflection or transmission (if the bottom surface is transparent), the asymmetry cannot be observed.

From the oscillation curve of the effective cavity, I_g is calculated by $I_g \sim A_e^2 \sin^2 \varphi_g$, which is plotted in Fig. 7. It can be seen that the asymmetry appears in the oscillation of I_g because of θ. Moreover, I_g and $\overline{|E_z|^2}$ almost overlap with each other. This confirms that the near field intensity is determined by I_g. Therefore, the asymmetry in I_g results in the asymmetric near-field oscillations.

Fig. 8 presents the field distribution of the case "M" and "N" marked in Fig. 3. M is a maximum of the asymmetric oscillations. The travelling wave is substantially distorted around the grating, and $|E_z|$ almost covers the whole active region, Fig. 8(a). While for the minimum "N", the incident light is nearly not affected by the grating, and $|E_z|$ is very weak as shown in Fig. 8(b). The two cases can be explained as follows. In the case "N", $\varphi_{gN} = \varphi_g$ (4.634 THz)$= \pi$, and thus $I_{gN} \sim A_e^2 \sin^2 \varphi_{gN} = 0$, which is seen in the distribution of $|E_x|$ in Fig. 8(b). The grating sits at the wave node of the standing wave, and the intensity around the grating is a minimum, leading to a weak coupling with the grating and a minimum in $|E_z|$. For the same reason, the case "M" reaches a maximum in $|E_z|$ because $I_{gM} \sim A_e^2 \sin^2 \varphi_{gM}$ is a maximum. Now, we can conclude that for the system where a pure standing wave (with a standing wave ratio of 1) is formed in the device, the minimum of $|E_z|$ always happens when destructive FP condition of the original cavity is satisfied, whereas the maximum of $|E_z|$ locates between the frequencies of $(A_e)_{\max}$ and $(A_o)_{\max}$. That is to say, the minimums are at $(A_o)_{\min}$, but the maximums are not at $(A_o)_{\max}$ (close to $(A_e)_{\max}$ in our system), which exhibits the asymmetry.

With these results, we find that a 614-μm-length GaAs slab can reproduce the photocurrent spectrum of V266-G15, which is plotted in Fig. 9.

IV. Conclusion

In conclusion, near-field asymmetric oscillations are found in a grating-coupled THzQWP system. Below the cutoff of the gratings, the near field is a result of the evanescent non-zeroth order diffracted modes. The intensity of the near field ($|E_z|^2$) is determined by the intensity of the incident light shining on the grating (I_g). In the system studied here, I_g is modulated by the FP cavity, and the cavity is coupled with the metal gratings where a reflection phase shift θ is introduced. By analyzing the field distribution, we find that θ plays an important role in the asymmetry. An effective FP cavity is formed due to the modified resonant condition by θ. Although the FP modes of the effective cavity are still symmetric, I_g no longer remains symmetric. This induces an asymmetric $|E_z|^2$, which is finally detected by the THzQWP.

Since THzQWPs are only sensitive to E_z which is directly related to the near field or surface modes, some near-field information can be extracted from the photocurrent spectra. Other coupling features between light and microstructures can also be detected provided E_z is changed at the coupling frequencies. Compared with far-field measurements, the direct detection of E_z by THzQWPs reflects the near-field information, such as the asymmetric oscillations. This confirms that the photocurrent measurement on a THzQWP could be an option to characterize the near-field properties of the microstructures on its surface.

References

[1] T. W. Ebbesen, H. J. Lezec, H. F. Ghaemi, T. Thio, and P. A. Wolff, "Extraordinary optical transmission through sub-wavelength hole arrays," *Nature*, vol. 391, no. 6668, pp. 667–669, Feb. 1998.

[2] L. Martin-Moreno, F. J. Garcia-Vidal, H. J. Lezec, K. M. Pellerin, T. Thio, J. B. Pendry, and T. W. Ebbesen, "Theory of extraordinary optical transmission through subwavelength hole arrays," *Phys. Rev. Lett.*, vol. 86, no. 6, pp. 1114–1117, Feb. 2001.

[3] J. A. Porto, F. J. Garcia-Vidal, and J. B. Pendry, "Transmission resonances on metallic gratings with very narrow slits," *Phys. Rev. Lett.*, vol. 83, no. 14, pp. 2845–2848, Oct. 1999.

[4] Q. Cao and P. Lalanne, "Negative role of surface plasmons in the transmission of metallic gratings with very narrow slits," *Phys. Rev. Lett.*, vol. 88, no. 5, pp. 057403-1–057403-4, Feb. 2002.

[5] J. B. Pendry, L. Martin-Moreno, and F. J. Garcia-Vidal, "Mimicking surface plasmons with structured surfaces," *Science*, vol. 305, no. 5685, pp. 847–848, Aug. 2004.

[6] M. Beruete, M. Navarro-Cía, and M. S. Ayza, "Understanding anomalous extraordinary transmission from equivalent circuit and grounded slab concepts," *IEEE Trans. Microw. Theory Tech.*, vol. 59, no. 9, pp. 2180–2188, Sep. 2011.

[7] M. Beruete, M. Navarro-Cía, S. A. Kuznetsov, and M. Sorolla, "Circuit approach to the minimal configuration of terahertz anomalous extraordinary transmission," *Appl. Phys. Lett.*, vol. 98, no. 1, pp. 014106-1–014106-3, Jan. 2011.

[8] V. Lomakin and E. Michielssen, "Enhanced transmission through metallic plates perforated by arrays of subwavelength holes and sandwiched between dielectric slabs," *Phys. Rev. B*, vol. 71, no. 23, pp. 235117-1–235117-10, Jun. 2005.

[9] M. Sarrazin, J. P. Vigneron, and J. M. Vigoureux, "Role of Wood anomalies in optical properties of thin metallic films with a bidimensional array of subwavelength holes," *Phys. Rev. B*, vol. 67, no. 8, pp. 085415-1–085415-8, Feb. 2003.

[10] F. J. G. de Abajo, "Colloquium: Light scattering by particle and hole arrays," *Rev. Mod. Phys.*, vol. 79, no. 4, pp. 1267–1290, Oct. 2007.

[11] D. Armand, Y. Todorov, F. Garet, C. Minot, and J. L. Coutaz, "Study of the transmission of subwavelength metallic grids in the THz frequency range," *IEEE J. Sel. Topics Quantum Electron.*, vol. 14, no. 2, pp. 513–520, Mar. 2008.

[12] C. Minot, Y. Todorov, D. Armand, F. Garet, and J. L. Coutaz, "Long-wavelength limit and Fano profiles of extraordinary transmission through metallic slit gratings in the THz range," *Phys. Rev. B*, vol. 80, no. 15, pp. 153410-1–153410-4, Oct. 2009.

[13] Y. Todorov and C. Minot, "Modal method for conical diffraction on a rectangular slit metallic grating in a multilayer structure," *J. Opt. Soc. Amer. A*, vol. 24, no. 10, pp. 3100–3114, Oct. 2007.

[14] R. Mueckstein, C. Graham, C. C. Renaud, A. J. Seeds, J. A. Harrington, and O. Mitrofanov, "Imaging and analysis of THz surface plasmon polariton waves with the integrated sub-wavelength aperture probe," *J. Infrared Milli. Terahertz Waves*, vol. 32, nos. 8–9, pp. 1031–1042, Aug. 2011.

[15] R. Zhang, X. G. Guo, C. Y. Song, M. Buchanan, Z. R. Wasilewski, J. C. Cao, and H. C. Liu, "Metal-grating-coupled terahertz quantum-well photodetectors," *IEEE Electron Device Lett.*, vol. 32, no. 5, pp. 659–661, May 2011.

[16] M. Patrashin and I. Hosako, "Terahertz frontside-illuminated quantum-well photodetector," *Opt. Lett.*, vol. 33, no. 2, pp. 168–170, Jan. 2008.

[17] H. C. Liu, M. Buchanan, and Z. R. Wasilewski, "How good is the polarization selection rule for intersubband transitions?" *Appl. Phys. Lett.*, vol. 72, no. 14, pp. 1682–1684, Apr. 1998.

[18] *Multiphysics Modeling and Simulation Software–COMSOL 4.2*. (May 18, 2011) [Online]. Available: http://www.comsol.com

[19] H. Luo, H. C. Liu, C. Y. Song, and Z. R. Wasilewski, "Background-limited terahertz quantum-well photodetector," *Appl. Phys. Lett.*, vol. 86, no. 23, pp. 231103-1–231103-3, Jun. 2005.

[20] R. Zhang, X. G. Guo, J. C. Cao, and H. C. Liu, "Near field and cavity effects on coupling efficiency of one-dimensional metal grating for terahertz quantum well photodetectors," *J. Appl. Phys.*, vol. 109, no. 7, pp. 073110-1–073110-5, Apr. 2011.

[21] J. S. Blakemore, "Semiconducting and other major properties of gallium arsenide," *J. Appl. Phys.*, vol. 53, no. 10, pp. R123–R181, May 1982.

[22] F. J. Garcia-Vidal and L. Martin-Moreno, "Transmission and focusing of light in one-dimensional periodically nanostructured metals," *Phys. Rev. B*, vol. 66, no. 15, pp. 155412-1–155412-9, Oct. 2002.

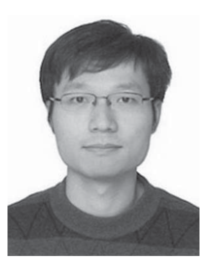

Rong Zhang was born in Nanjing, China. He received the Bachelors degree in biological physics from Nanjing University, Nanjing, in 2006, and the Doctoral degree in microelectronics and solid-state electronics from the Shanghai Institute of Microsystem and Information Technology (SIMIT), Chinese Academy of Sciences, Shanghai, China, in 2011.

He is currently an Assistant Researcher with the Key Laboratory of Terahertz Solid-State Technology, SIMIT. His current research interests include terahertz semiconductor devices and their applications.

Xuguang Guo was born in Liaoning, China. He received the Bachelors and Masters degrees in physical electronics from Fudan University, Shanghai, China, in 1997 and 2000, respectively, and the Ph.D. degree in microelectronics and solid-state electronics from the Shanghai Institute of Technical Physics, Chinese Academy of Sciences, Shanghai, in 2003.

He is currently a Professor with the Key Laboratory of Terahertz Solid-State Technology, Shanghai Institute of Microsystem and Information Technology, Chinese Academy of Sciences. His current research interests include terahertz semiconductor optoelectronic devices.

Juncheng Cao was born in Jiangxi, China, in 1967. He received the Ph.D. degree in electrical engineering from Southeast University, Nanjing, China, in 1994.

He is currently the Terahertz (THz) Group Leader and the Director of the Key Laboratory of Terahertz Solid-State Technology, Shanghai Institute of Microsystem and Information Technology, Chinese Academy of Sciences, Shanghai, China. From 1999 to 2000, he was a Senior Visiting Scientist with the National Research Council, Ottawa, ON, Canada. He and his group members successfully developed a THz quantum cascade laser and its applications in THz communication and imaging, developed Monte Carlo simulation method for THz quantum cascade lasers, developed THz-radiation-induced semiconductor impact ionized model, and successfully explained the absorption of strong THz irradiation in low-dimensional semiconductor. His current research interests include THz semiconductor devices and their applications.

Dr. Cao was a recipient of the National Fund for Distinguished Young Scholars of China and the Natural Science Award of Shanghai (the Peony Award) in 2004. He was the recipient of the Excellent Teacher Award from the Chinese Academy of Sciences in 2006 and 2011.

Huichun Liu (M'99–SM'05–F'07) was born in Taiyuan, China. He received the B.Sc. degree in physics from Lanzhou University, Lanzhou, China, in 1982, and the Ph.D. degree in applied physics from the University of Pittsburgh, Pittsburgh, PA, in 1987, as an Andrew Mellon Predoctoral Fellow.

He was with the Institute for Microstructural Sciences, National Research Council, Ottawa, ON, Canada, from 1987 to 2011. He is currently with Shanghai Jiao Tong University, Shanghai, China, as a "1000" Chair Professor. He has published extensively in refereed journals with an H-index of 38 and has presented more than 90 plenary and invited talks in international conferences. His current research interests include semiconductor quantum devices.

Dr. Liu has been a fellow of the Academy of Sciences, Royal Society of Canada and the American Physical Society. He was the recipient of the Herzberg Medal from the Canadian Association of Physicists in 2000, the Bessel Prize from the Alexander von Humboldt Foundation in 2001, the Distinguished Young Scientist Award from the NSFC-B in 2005, and the Changjiang Scholar Award in 2008.